

Observation of excitonic transitions in InSb quantum wells

N. Dai, F. Brown, P. Barsic, G. A. Khodaparast, R. E. Doezema, M. B. Johnson, S. J. Chung, K. J. Goldammer, and M. B. Santos

Department of Physics and Astronomy and Laboratory for Electronic Properties of Materials, The University of Oklahoma, Norman, Oklahoma 73019

(Received 30 March 1998; accepted for publication 30 June 1998)

We report the observation of interband exciton transitions in InSb/Al_xIn_{1-x}Sb multi-quantum-well samples. The exciton peaks are identified with the use of a simple quantum well model. The strain present in the InSb wells alters the spectrum significantly from that for unstrained III-V materials and makes it possible to use the exciton spectrum in determining the band offset. © 1998 American Institute of Physics. [S0003-6951(98)01934-2]

Since the advent of the first band-gap engineered materials, optical transitions corresponding to interband excitations have been highly useful in understanding confinement-induced band structure in semiconductors.¹⁻³ In this letter we report the first observation of the interband exciton spectrum in InSb quantum wells. Because of its narrow energy gap and small effective mass, InSb has the highest intrinsic electron mobility of all binary III-V compounds; thus InSb quantum wells can potentially be fabricated into specialized photonic and high speed electronic devices. Of special interest in our strained-layer samples are the qualitative changes in the exciton spectrum compared to unstrained III-V quantum wells. The altered exciton spectrum is similar to that observed in the strained In_xGa_{1-x}As/GaAs system.⁴

Our samples are multi-quantum-well (MQW) InSb/Al_xIn_{1-x}Sb heterostructures grown on GaAs substrates.⁵ For the measurements described here, we have chosen a sequence of 25 nominally undoped InSb MQWs with well thickness $d=250$ Å. The alloy barriers are 500 Å thick with Al concentration $x=0.09$. We use a Fourier transform infrared (FTIR) spectrometer to monitor the sample transmission as a function of photon frequency ν . To reduce unwanted Fabry-Perot interference, we have coated the top surface of the sample with an antireflection NiCr film.⁶ Figure 1 shows the transmission, T_{MQW} , of a MQW sample referenced to the transmission, T_{sub} , of a sample with a similar substrate and epitaxial layer but lacking the InSb MQW sequence. Above the InSb band-gap energy (236 meV in unstrained bulk InSb),⁷ the spectrum shows absorption structures characteristic of excitonic continuum absorption between the stepped density of states for two-dimensional confined valence and conduction band states and the discrete exciton peaks at the step onsets.

The onset structures are enhanced by plotting the difference between a 4.2 K spectrum and that at a higher temperature (22 K), as in Fig. 2. This differential spectrum is made possible by the temperature dependence of the InSb band gap. The 4.2 K gap of 236 meV is reduced to 228 meV at 80 K, thus for the temperature difference of Fig. 2, a linear variation of energy gap with temperature predicts that the energy gap differential is about 2 meV. This differential enhancement technique gives essentially the negative derivative of the exciton structure in Fig. 1. We have checked this by numerically calculating the derivative of the 4.2 K transmission curve of Fig. 1. The 3D peak for a thick (5.7 μm)

InSb epitaxial layer on GaAs is also shown in the figure. This peak is observed at the accepted 236 meV value of the band-gap energy since the exciton binding energy is expected to be small (~ 0.4 meV) due to the small effective mass in the conduction band.

In our MQW structures, the bulk InSb band gap is altered because of the strain caused by the pinning of the in-plane lattice constant in the InSb layers to the lattice constant of the barriers. Assuming a linear variation with alloy concentration, the strain is given by

$$\epsilon_{\parallel} = \frac{a' - a}{a} x, \quad (1)$$

where a and a' are the InSb and AlSb lattice constants, 6.47 and 6.136 Å, respectively.⁷ The strain modifies the unstrained band-gap E_g to the values E'_{\pm} given to first order in ϵ_{\parallel} by⁸

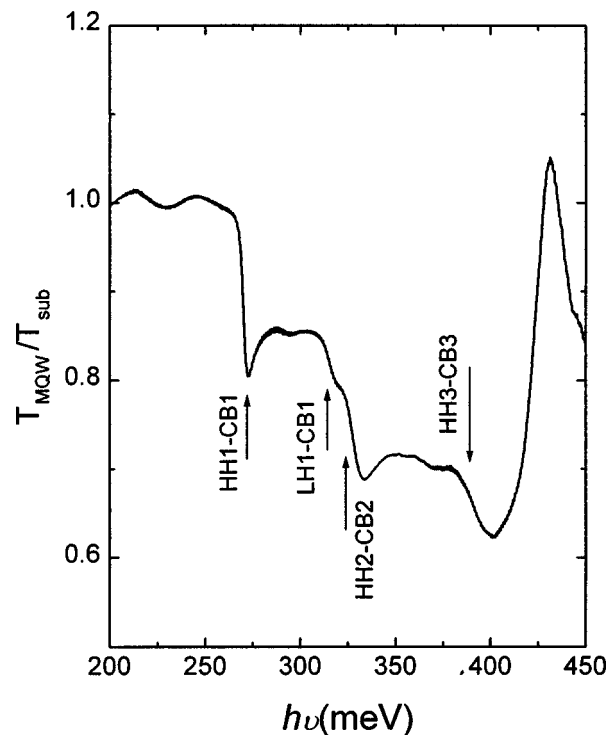


FIG. 1. Transmission spectrum of InSb/Al_{0.09}In_{0.91}Sb MQW sample at 4.2 K. The ratio of the transmission of the MQW sample to that of a reference sample lacking the MQWs is plotted vs. photon energy. Calculated transition energies are marked.

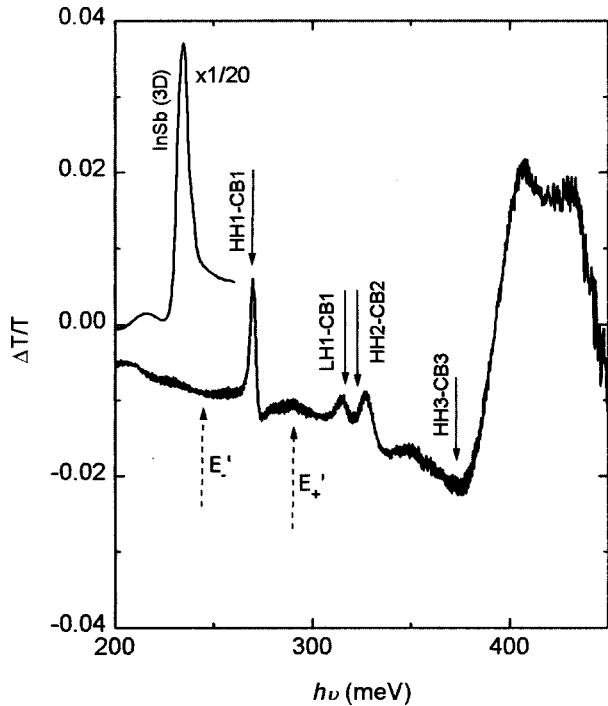


FIG. 2. Differential transmission spectrum of an InSb/Al_{0.09}In_{0.91}Sb MQW sample. The transmission difference, $T_{\text{MQW}}(4.2 \text{ K}) - T_{\text{MQW}}(22 \text{ K})$ relative to the average transmission T is plotted vs photon energy. Calculated transition energies and band gaps are indicated.

$$E'_{\pm} = E_g + \left[\alpha \left(2 - 2 \frac{C_{12}}{C_{11}} \right) \pm \beta \left(1 + 2 \frac{C_{12}}{C_{11}} \right) \right] \epsilon_{\parallel}, \quad (2)$$

where α is the sum of the conduction and valence band deformation potentials, β is the shear deformation potential, and the C_{ij} are the elastic constants. (We use Landolt-Börnstein⁷ values for all these quantities.) The + sign gives the gap between the conduction band and the light-hole band and the - sign the gap between the conduction band and the heavy-hole band. In our case of compressive strain, therefore, the light-hole gap is larger than the heavy-hole gap. For $x=0.09$, the heavy-hole and light-hole gaps are shown in Fig. 2.

To model the electronic band structure of the quantum wells, we must introduce the band-offset ratio, Q_c , which is not known for the InSb/Al_xIn_{1-x}Sb system.⁹ We define Q_c as the fraction of the minimum band-gap discontinuity which appears in the conduction band at the InSb-Al_xIn_{1-x}Sb boundary; thus, in our samples, Q_c is the offset ratio for the conduction and heavy-hole bands.

Figure 3 shows the conduction and valence band quantum wells for $Q_c=0.70$ for a 250 Å thick InSb layer with Al_{0.09}In_{0.91}Sb barriers. For the light-hole band gap, we have included the correction term to Eq. (2) which is proportional to the square of the strain.⁸ The electron and light-hole subband edges were calculated in the two-band approximation¹⁰ to take the extreme nonparabolicity of these bands in InSb into account and we used a parabolic dispersion for the heavy holes. These approximations should be quite adequate for the conduction and heavy-hole bands; the light-hole quantum well is so shallow that the exact location of the bound state is not crucial in calculating the interband transitions. The band-edge masses are taken to be 0.0139, 0.015,

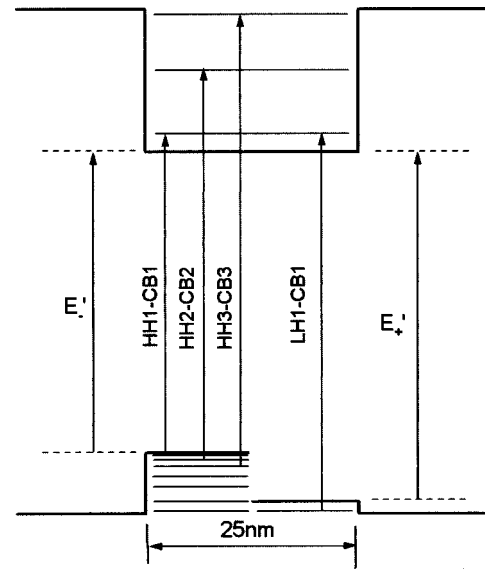


FIG. 3. Conduction and valence band edges for an InSb/Al_{0.09}In_{0.91}Sb quantum well with a band offset ratio of $Q_c=0.70$.

and 0.47 for the electrons, light holes, and heavy holes, respectively, in free electron units. Band-edge effective mass values in the alloy are assumed to vary with $E_g(x)$ according to the Kane model. The energy gap in the alloy is taken to vary with concentration x as $E_g(x) = E_g(0) + (2.0 \text{ eV})x$.^{7,11} The uncertainty in the slope, 2.0 eV, is about 5%; thus the gap value for $x=0.09$ has an uncertainty of about 2%.

With the selection rule,² $\Delta n=0$ (where n is the subband index), the calculation predicts three transitions: three heavy-hole transitions to the three conduction-band subbands and one transition from the single light-hole subband to the conduction band. The predicted transition energies shown in Fig. 3 are also marked in Figs. 1 and 2. The close agreement with the experimental peaks suggests that we have correctly identified the transitions. Because the highest lying subband is so weakly bound, we do not expect to be able to distinguish transitions to this subband from transitions to the continuum; indeed, the predicted position of the HH3-CB3 transition marks the onset of a broad absorption band. We ascribe the absorption structure near 430 meV to interband transitions across the gap of the Al_xIn_{1-x}Sb barrier. If this value corresponds to the alloy gap, the $E_g(x)$ relation, given above from Refs. 7 and 11, predicts an Al concentration of 9.7%. We intend a careful future study of the alloy absorption structure as a function of concentration.

Especially noteworthy is the position of the light-hole transition (LH1-CB1). This transition is seen in GaAs quantum wells very near the heavy-hole ground-state subband transition (HH1-CB1). Its shift to near the HH2-CB2 position is a consequence of the strain-induced difference between the band gaps for the light and heavy holes. As in the similar In_xGa_{1-x}As/GaAs system, Eq. (2) (corrected by the small, quadratic term⁸ in ϵ_{\parallel}) predicts that, for offset ratios larger than 0.77, there is no potential well for light holes in the InSb. Thus for offset ratios larger than 0.77, the system of light holes and electrons is predicted to become type II. The offset ratio at which the transition occurs is nearly independent of concentration x since both the strain ϵ_{\parallel} and the alloy band-gap $E_g(x)$ vary linearly with x and thus only

through the small correction term to Eq. (2), which is quadratic in ϵ_{\parallel} , does a weak concentration dependence occur.

The uncertainties in the offset ratio and in the alloy band gap give an associated uncertainty in the confinement potentials for electrons and holes. In view of this, using a more sophisticated model² for the confined states is not warranted at this time, but we hope to be able to determine the alloy band gap more accurately as a function of concentration using transmission measurements in the MQW samples. The sensitivity of the LH1-CB1 transition to the offset¹² as the thickness d is varied should allow us to determine the offset-ratio for the InSb/Al_xIn_{1-x}Sb system in conjunction with a four-band calculation.² This will require line shape identification of the exact transition energies, a subject we have avoided here. Early analysis with the four-band calculation suggests that the band offset ratio is lower than the value, 0.70, used here and could be as low as 0.55. Another study we hope to report in the near future is that of the exciton spectrum for doped samples.

This work is supported by NSF Grant Nos. DMR-9624699 and OSR-9550478.

- ¹R. Dingle, in *Festkörperprobleme*, edited by H. J. Queisser, Adv. Solid State Phys., Vol. 15 (Pergamon/Vieweg, Braunschweig, 1975), p. 21.
- ²G. Bastard, *Wave Mechanics Applied to Semiconductor Heterostructures* (Les Editions Physique, Les Ulis, 1988).
- ³K. Ploog, in *Excitons in Confined Systems*, edited by R. Del Sole, A. D'Andrea, and A. Lapicciarella, Springer Proceedings in Physics (Springer, Berlin, Heidelberg, 1988), p. 120.
- ⁴J.-Y. Marzin, M. N. Charasse, and B. Sermage, Phys. Rev. B **31**, 8298 (1985).
- ⁵W. K. Liu, X. Zhang, W. Ma, J. Winesett, and M. B. Santos, J. Vac. Sci. Technol. B **14**, 2339 (1996); and K. J. Goldammer, W. K. Liu, G. A. Khodaparast, S. C. Lindstrom, M. B. Johnson, R. E. Doezema, and M. B. Santos, *ibid.* (in press).
- ⁶S. W. McKnight, K. P. Stewart, H. D. Drew, and K. Moorjani, Infrared Phys. **27**, 327 (1987).
- ⁷Landolt-Börnstein, in *Numerical Data and Functional Relationships in Science and Technology*, edited by O. Madelung, Group III, Vol. 17 (Springer, Berlin, 1982).
- ⁸S. R. Kurtz and R. M. Biefeld, Phys. Rev. B **44**, 1143 (1991).
- ⁹M. K. Saker, D. M. Whittaker, M. S. Skolnick, C. F. McConville, C. R. Whitehouse, S. J. Barnett, A. D. Pitt, A. G. Cullis, and G. M. Williams, Appl. Phys. Lett. **65**, 1118 (1994).
- ¹⁰For example, R. E. Doezema and H. D. Drew, Phys. Rev. Lett. **57**, 762 (1986).
- ¹¹Ya. Agaev and N. G. Bekmedova, Sov. Phys. Semicond. **5**, 1330 (1972).
- ¹²G. Ji, D. Huang, U. K. Reddy, T. S. Henderson, R. Houdre, and H. Morkoç, J. Appl. Phys. **62**, 3366 (1987).